

Diethylenetriamine-assisted one-step hydrothermal synthesis of cotton-like CoS cluster for high-performance supercapacitor

JIA ZHU^{1,2}, LEI XIANG², YAZHOU ZHOU¹, JUAN YANG^{1,*}

¹School of Materials Science and Engineering, Jiangsu University, Zhenjiang 212013, PR China

²School of Environmental and Chemical Engineering, Jiangsu University of Science and Technology, Zhenjiang 212003, PR China

Cotton-like CoS cluster has been successfully synthesized via a simple one-step hydrothermal route assisted by diethylenetriamine (DETA) as a ligand and structure-directing agent. The structure and morphology of the product were characterized by X-ray diffraction (XRD), transmission electron microscopy (TEM), field emission scanning electron microscopy (FE-SEM) and N₂ adsorption-desorption isotherm. The CoS sample which has a hexagonal phase without any impurities possesses a microscopic morphology made by cotton-like clusters. The as-fabricated CoS as a supercapacitor electrode presents desirable supercapacitive performance with a high specific capacitance (664 F·g⁻¹ at 0.5 A·g⁻¹), remarkable rate capability and excellent cycling stability (85.7 % specific capacitance retention after 1000 cycles), making it applicable as an electrode for high-performance supercapacitors.

Keywords: cobalt sulfide; diethylenetriamine; hydrothermal synthesis; supercapacitor; pseudocapacitance

1. Introduction

With the increasing energy consumption and global warming, it is urgent to search for sustainable and alternative energy conversion and storage devices [1–3]. Supercapacitors, also named electrochemical capacitors (ECs) have received a lot of interests due to their prominent features of rapid charging-recharging rate, long durability, high power density and eco-friendliness [4, 5]. In terms of charge storage mechanism, ECs can be normally sorted into two types, pseudocapacitors relied on Faradic reactions of the modified-electrode and electrical double-layer capacitors (EDLCs) involved in charge absorption and diffusion at electrode/electrolyte interface [6].

As is well-acknowledged, electrochemical performances of functional materials depend strongly on their size, morphology and architecture. Functional materials with novel cotton-shaped architecture have served as photocatalysts, biosensors

and adsorbents [7–9]. Many researchers have focused on rational designing desirable porous structures, novel heterostructures and complicated hierarchical structures of the electrode materials to further enhance the capacitive properties [10, 11]. For example, the strategy of introducing structure-directing agents or ligands has been extensively employed to generate effectively electroactive materials with special structures [12–14].

Among transition metal chalcogenides, cobalt sulfide materials with various stoichiometric compositions, such as CoS, CoS₂, Co₃S₄, Co₈S₉ have been widely explored as supercapacitors. Specifically, CoS is considered as a promising candidate for supercapacitors due to its high reversible redox capability as well as cost effectiveness [15, 16]. CoS electrode materials fabricated by different methods have diverse nanostructures or microstructures and exhibit attractive electrochemical properties. For instance, CoS microspheres [17] are produced in mixed solvents through benign hydrothermal route. CoS nanosheets [18] electrochemically deposited on nickel foam could

*E-mail: yangjuan6347@ujs.edu.cn

exhibit a high specific capacitance of $1471 \text{ F}\cdot\text{g}^{-1}$ at $4 \text{ A}\cdot\text{g}^{-1}$ in 1 M KOH aqueous electrolyte. Hollow CoS nanoprisms [19] have been prepared by a two-step and microwave-assisted method. Despite manifold alternative synthesis ways to obtain CoS supercapacitors with multiple nanostructure and microstructure, it still remains an expectation for seeking a simple and efficient approach to acquire cotton-like CoS supercapacitor since this special structure facilitates an easy contact between electrolyte and electrode, thus improving the electrode material utilization rate and capacitance performance [20].

Herein, we report an easy one-step hydrothermal strategy to fabricate high purity cotton-like CoS cluster with the aid of diethylenetriamine (DETA) as a ligand and structure-directing agent. Benefiting from its synergic properties of metallic compound nature and cotton-like microstructure, the CoS-modified electrode as supercapacitor showed a typical pseudocapacitance behavior with a high specific capacitance of $664 \text{ F}\cdot\text{g}^{-1}$ at $0.5 \text{ A}\cdot\text{g}^{-1}$, remarkable rate capability and excellent cycling stability with 85.7% specific capacitance retention after 1000 cycles, offering promising application in supercapacitor.

2. Experimental

2.1. Preparation of cotton-like CoS clusters

All reagents were of analytical grade and used as received. Cotton-like CoS clusters were prepared as follows: $0.15 \text{ g Co}(\text{CH}_3\text{COO})_2\cdot 4\text{H}_2\text{O}$ and $0.0905 \text{ g thioacetamide (TAA)}$ were dispersed in 20 mL distilled water under stirring. After 30 min , $300 \mu\text{L DETA}$ was added to the mixture. Stirred vigorously for 1 h , the mixture was transferred into a 25 mL Teflon-lined autoclave for hydrothermal treatment at $180 \text{ }^\circ\text{C}$ for 12 h . After being cooled down to room temperature, the precipitates were separated by centrifugation and rinsed with distilled water and absolute ethanol for several times to remove the residues. The final CoS product was vacuum dried at $60 \text{ }^\circ\text{C}$ for 10 h . For comparison, the material was fabricated by the same hydrothermal process in absence of diethylenetriamine.

2.2. Characterization

The microstructure and morphology of the obtained material were observed by field-emission scanning electron microscopy (FE-SEM, JEOL JSM-7100F) and transmission electron microscopy (TEM, JEOL 2010) using an accelerating voltage of 200 kV . The crystal structure was analyzed by powder X-ray diffraction with $\text{CuK}\alpha$ radiation (XRD, Rigaku Dmax 2500 PC). The specific surface area calculated by Brunauer-Emmett-Teller (BET) method was recorded on N_2 adsorption-desorption analyzer at 77 K (ASAP 2020).

2.3. Electrochemical measurements

To evaluate the electrochemical performances of the resultant CoS material, a three-electrode cell in 6 M KOH aqueous electrolyte was employed. Working electrodes based on CoS material were prepared by thorough mixing $80 \text{ wt.}\%$ CoS material, $10 \text{ wt.}\%$ carbonblack and $10 \text{ wt.}\%$ polytetrafluoroethylene (PTFE) binder into a slurry. The slurry was loaded onto Ni foam ($1 \text{ cm} \times 1 \text{ cm}$) and pressed at 10 MPa . After vacuum drying at $80 \text{ }^\circ\text{C}$ for 10 h , CoS-modified electrode was obtained. The mass of the electroactive material loading in Ni foam was approximately 1.5 mg . Platinum foil and saturated calomel electrode (SCE) acted as counter and reference electrodes, respectively. The electrochemical studies including cyclic voltammetry (CV), galvanostatic charge/discharge (GCD) and electrochemical impedance spectroscopy (EIS) were carried out on a CHI760E electrochemical work station (Shanghai, China). Cycling performance was measured with a CT 2001A Tester (Wuhan, China).

The specific capacitance established by galvanostatic charge-discharge (GCD) method can be calculated from the equation [21]:

$$C = I \cdot \Delta t / (m \cdot \Delta V) \quad (1)$$

where C ($\text{F}\cdot\text{g}^{-1}$) is specific capacitance, I (A) is discharging current, Δt is discharge time, ΔV is potential drop, and m (g) is mass of electroactive material on the working electrode.

3. Results and discussion

As we know, Co^{2+} tends to cooperate with amine ligand to form a sexadentate complex compound [22, 23]. Among a variety of ligands, diethylenetriamine is a significant amine ligand for the synthesis of several functional materials [24–26]. For the growth of cotton-like CoS clusters assisted by DETA, a possible process can be described as follows. Firstly, Co^{2+} reacted with DETA to produce dark red complex. With rising temperature, S^{2-} could release slowly as TAA decomposed. Then, the generated S^{2-} gradually grabbed Co^{2+} in the complex to produce CoS nucleus. Consequently, through the well-known Ostwald ripening process, the CoS crystallites afterwards grew into cotton-like CoS clusters. During the hydrothermal process, DETA reduced the concentration of free Co^{2+} by effective coordination with Co^{2+} . Moreover, the gradual generation of S^{2-} occurred as the decomposition of TAA and restricted the growth and cohesion of the crystal. This is in favor of the formation of cotton-like CoS clusters.

3.1. XRD patterns and BET specific surface area analysis

Fig. 1a displays the XRD pattern of CoS product. The diffraction peaks at $2\theta = 30.6^\circ$, 35.3° , 46.9° and 54.4° unambiguously correspond to respective (1 0 0), (1 0 1), (1 0 2) and (1 1 0) planes of CoS. All the diffraction peaks are in good agreement with the standard hexagonal CoS with the lattice parameters $a = b = 3.368 \text{ \AA}$, $c = 5.17 \text{ \AA}$ (JCPDS Card No. 65-3418). No other peaks from other phases were detected, implying high purity and single-phase crystallization of the product. Additionally, the weak intensity of diffraction peaks reflects weak crystallinity of the sample. As is shown in Fig. 1b, the XRD pattern of the product obtained without the aid of diethylenetriamine is different from that of CoS (JCPDS Card No. 65-3418) and cannot be indexed to any single JCPDS Card, certifying the poor crystalline properties of the product. These results indicate that the effect of diethylenetriamine in the hydrothermal process plays a key role in the preparation and crystalline properties of CoS clusters.

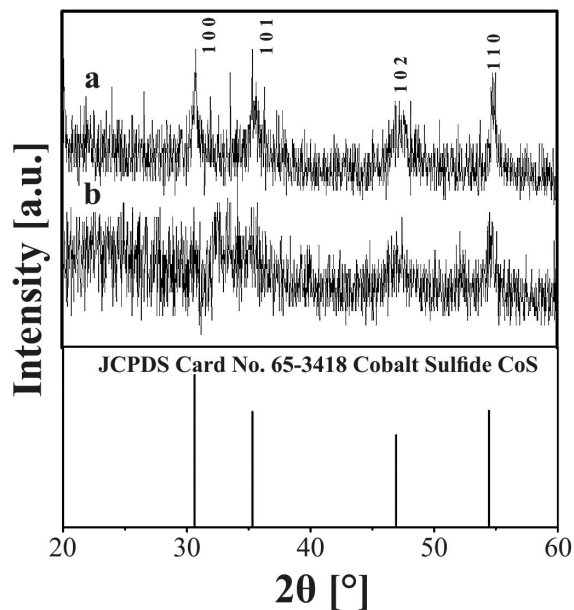


Fig. 1. XRD patterns of (a) cotton-like CoS obtained at presence of diethylenetriamine and (b) product obtained in absence of diethylenetriamine.

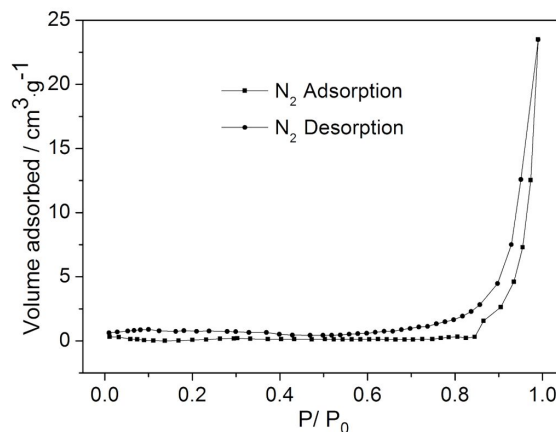


Fig. 2. N_2 adsorption-desorption isotherms of cotton-like CoS.

The N_2 adsorption-desorption isotherms plot of as-prepared CoS is shown in Fig. 2. The plot reveals a representative IV isotherm with an apparent hysteresis loop starting from $P/P_0 = 0.02$. The BET surface area and total pore volume of cotton-like CoS were determined to be $2.80 \text{ m}^2 \cdot \text{g}^{-1}$ and $0.036 \text{ cm}^3 \cdot \text{g}^{-1}$. These relatively low values authenticate the typical large cotton-like clusters characteristic of CoS product.

3.2. Morphology and microstructure

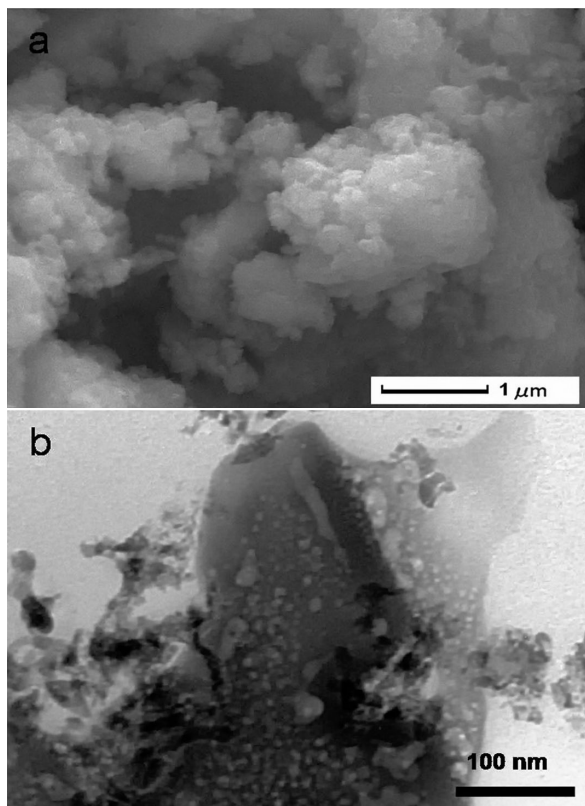


Fig. 3. SEM (a) and TEM (b) images of cotton-like CoS.

The SEM image in Fig. 3a reveals the closely packed and interconnected cotton-like microscopic morphology of CoS sample. Evidently, the cotton-like CoS clusters exhibit coarse and uneven surface. Such microstructure favors the formation of an interlinked conducting network, which contributes to fast electron transfer and ion diffusion between electrolyte and CoS electrode. The TEM micrograph depicted in Fig. 3b further verifies the microstructure of the CoS. In accordance with the SEM observations, the sample presents densely stacked and aggregated arrangement of groups of clusters with irregular sizes. This special cotton-like microstructure leads to a limited BET specific surface area of $2.80 \text{ m}^2 \cdot \text{g}^{-1}$.

3.3. Electrochemical measurements

Cyclic voltammograms (CVs) of CoS-modified electrode at various scan rates are illustrated in

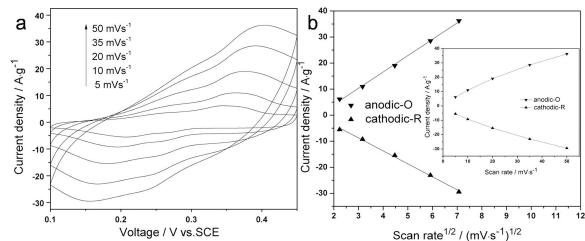


Fig. 4. (a) CV curves of CoS electrode at different scan rates; (b) plot of peak current vs. square root of scan rate and plot of peak current vs. scan rate (inset) of CoS electrode.

Fig. 4a. Apparently, there exists a pair of strong redox peaks in the CV curve, suggesting typical pseudocapacitance feature governed by reversible Faradaic reactions within the electrochemical process. The Faradaic reactions are likely to involve the reversible conversions of $\text{CoS} \rightleftharpoons \text{CoSOH}$ and $\text{CoSOH} \rightleftharpoons \text{CoSO}$. Furthermore, the shape of the CV curves demonstrates that the pseudocapacitance characteristic of CoS-modified electrode is distant from that of EDLC, whose CV curve is similar to an ideal rectangle [27]. According to the literature [18, 28], two redox reactions of the CoS electrode in KOH electrolytes are expressed as follows:



and



As scan rate elevates from $5 \text{ mV} \cdot \text{s}^{-1}$ to $50 \text{ mV} \cdot \text{s}^{-1}$, the potentials of anodic and cathodic peaks move to more positive and negative directions respectively. This occurs because internal diffusion resistance in the pseudoactive electrode material increases with the augmentation of scan rate [29, 30]. Also the peak current densities I_p rise by enlarging scan rate V . This is owing to the limited ion diffusion rate failing to neutralize electronic during Faradic reactions [31]. Originated from the CV curves, Fig. 4b shows a good linearity between oxidation and reduction I_p against $V^{1/2}$. As Sevcik equation describes, in semi-infinite diffusion process relying on CV in liquid electrolytes,

I_p vs. $V^{1/2}$ gives a linear relationship for a kinetically plain redox reaction regardless of the scan rate [32]. Contrarily, I_p vs. V is a non-linear relationship in the inset of Fig. 4b. I_p vs. V is supposed to be linear for the charge absorption and accumulation process of EDLC [27]. These results confirm that the diffusion process of hydroxyl ions actually governs the rate of redox reactions on CoS-modified electrode.

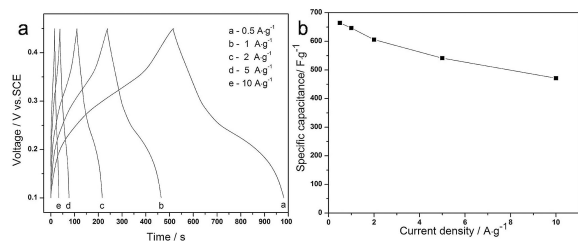


Fig. 5. (a) GCD curves of CoS electrode at different current densities; (b) specific capacitances of CoS electrode as a function of current density.

Fig. 5a presents the GCD curves of CoS electrode at diverse current densities. During charge-discharge process, a distinct plateau region and a non-linearity of potential vs. time in GCD curves signify typical pseudocapacitance characteristics derived from Faradic reactions between the electrode and electrolyte. This analysis agrees well with the result from the CV curves. Moreover, GCD configurations display high symmetry at different current densities, illustrating remarkable pseudocapacitance behavior and good reversible Faradic reaction capability. Based on equation 1, the specific capacitance of CoS product is calculated as 664, 647, 606, 541 and 471 $F \cdot g^{-1}$, when the current density is 0.5 $A \cdot g^{-1}$, 1 $A \cdot g^{-1}$, 2 $A \cdot g^{-1}$, 5 $A \cdot g^{-1}$ and 10 $A \cdot g^{-1}$, respectively (Fig. 5b). The value of specific capacitance is considered very high for pseudocapacitance performance, especially in view of the limited BET surface area ($\sim 2.80 \text{ m}^2 \cdot g^{-1}$). Meanwhile, this specific capacitance is higher than those of CoS microspheres ($363 \text{ F} \cdot g^{-1}$) [17], CoS nanoprisms ($224 \text{ F} \cdot g^{-1}$) [19] and CoS nanosheet ($318 \text{ F} \cdot g^{-1}$) [33]. Even at 10 $A \cdot g^{-1}$, CoS modified-electrode still offers $471 \text{ F} \cdot g^{-1}$, which maintains approximately 71 % of the specific capacitance at 0.5 $A \cdot g^{-1}$, indicating

excellent rate capability. It can be ascribed to synergic effects combining metallic compound intrinsic nature and cotton-like microstructure.

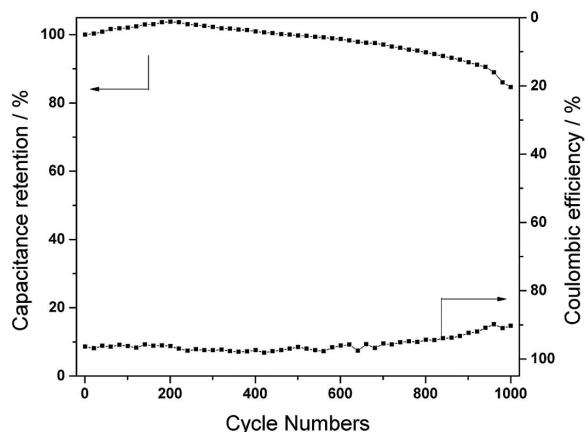


Fig. 6. Cycling performance and Coulombic efficiency of CoS electrode at 0.5 $A \cdot g^{-1}$.

The cycling performance including specific capacitance retention and Coulombic efficiency η [34] upon prolonged cycling was assessed by consecutive charge-discharge measurement at 0.5 $A \cdot g^{-1}$. As shown in Fig. 6, in the first 200 cycles the specific capacitance increases gradually from $664 \text{ F} \cdot g^{-1}$ to $689 \text{ F} \cdot g^{-1}$, which could be attributed to the full activation stemming from sufficient electrolyte permeation and wetting. In the last 800 cycles, the specific capacitance slightly decreases and about 86 % of the original value retains after 1000 cycles. Additionally, η , also called charge-discharge efficiency, preserves $>91 \%$ during the whole cycling process, indicating full activation and a high efficiency of the CoS-modified electrode. This excellent stability and high efficiency verify high reversibility of pseudocapacitance reactions between CoS pseudocapacitor and KOH electrolyte.

For understanding the fundamental supercapacitive behavior of as-prepared CoS electrode, EIS tests were performed in the frequency range of 0.1 Hz to 10 kHz at open circuit potential with a fixed amplitude of 5 mV. The Nyquist plots of CoS-modified electrode before and after 50 cycles are compared in Fig. 7. Both Nyquist plots share similar shape with two components containing

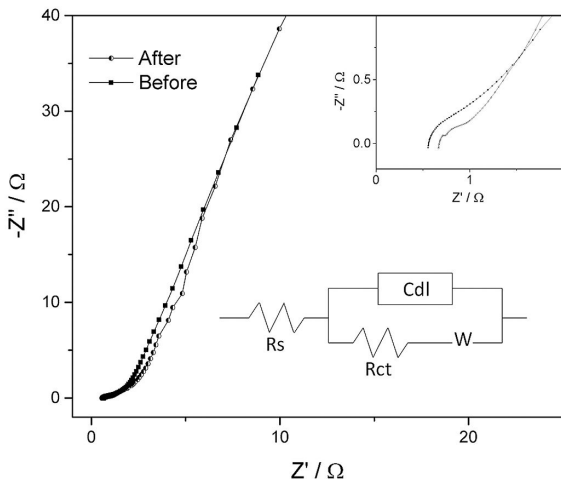


Fig. 7. Nyquist plots for CoS electrode before and after cycling. The inset shows the magnified plots in high frequency region and the equivalent circuit used to simulate the Nyquist plots.

a small depressed semicircle in high frequency region and a sloped line in low frequency region, indicating the high stability of CoS-modified electrode. On the basis of equivalent circuit model (inset of Fig. 7), the x-axis intercept in high frequency region is normally a representative of solution resistance R_s , which is a total resistance of inherent electrode resistance and contact resistance at electrolyte/electrode interfaces. Accordingly, the R_s value after cycling is 0.55Ω , which is smaller than 0.67Ω before cycling. The lower R_s value after cycling may be ascribed to the reduction of inner electrode resistance and contact resistance after the sufficient redox reaction and activation between electrolyte and electroactive material, which leads to efficiently accessible pathways in electrolyte to electrode surface. In high-medium frequency region, the span of the depressed semicircle determines charge transfer resistance R_{ct} of electrochemical process. R_{ct} is also called Faradaic resistance [35], determining the response rate of electrode material in electrolyte. It is widely accepted that smaller R_{ct} value is indeed associated with higher specific capacitance [36]. This result is in accordance with the analysis of Fig. 6 that the specific capacitance increases a little after 50 cycles. At high discharging current density, small R_s

and R_{ct} benefit from large specific capacitance for the enhancement of rate capability [27]. In low frequency region, the straight line corresponds to Warburg impedance W derived from ions diffusion from electrolyte to electrode interface. The high slope of the straight line belonging to CoS-modified electrode testifies faster ion transfer rates between the electrode and electrolyte. In addition, the nearly vertical linear part in the EIS spectra signifies the high capacitive behavior, an ideal capacitor model and electrochemical stability of the as-obtained CoS electrode [37]. Overall, the results manifest that CoS-modified electrode has favorable charge-transfer kinetics and fast ions transport rates, thus presenting the excellent pseudocapacitance performance.

4. Conclusion

A simple one-step hydrothermal method with the assistance of diethylenetriamine as a ligand and structure-directing agent has been applied to the fabrication of high purity cotton-like CoS clusters. Serving as electrode for supercapacitor, the cotton-like CoS cluster exhibits typical pseudocapacitance features and remarkable rate capability. The specific capacitance reaches the value as high as $664 \text{ F}\cdot\text{g}^{-1}$ at $0.5 \text{ A}\cdot\text{g}^{-1}$. Besides, CoS-modified electrode shows excellent cycling durability with about 86 % specific capacitance retention of its initial value after 1000 cycles. Such facile DETA-assisted hydrothermal synthesis approach can be extended to design other electrode materials for supercapacitors.

Acknowledgements

This work was financially supported by the Natural Science Foundation of China (51572114, 51672112).

References

- [1] SUN M.C., SUN M.F., YANG H.X., SONG W.H., SUN S.N., *Ceram. Int.*, 43 (2017), 363.
- [2] ZHANG J.H., KONG Q.H., YANG L.W., WANG D.Y., *Green Chem.*, 18 (2016), 3066.
- [3] KONG X.W., ZHANG R.L., ZHONG S.K., WU L., *Mater. Sci.-Poland*, 34 (2016), 227.
- [4] SHARMA P., BHATTI T.S., *Energ. Convers. Manage.*, 51 (2010), 2901.
- [5] SIMON P., GOGOTSI Y., *Nat. Mater.*, 7 (2008), 845.

- [6] WINTER M., BRODD R.J., *Chem. Rev.*, 4245 (2004), 104.
- [7] YU X., LI Z.H., LIU J.W., HU P.A., *Appl. Catal. B-Environ.*, 205 (2017), 271.
- [8] HU Y.Z., WANG X.X., ZOU Y.D., WEN T., WANG X.L., ALSAEDI A., HAYAT T., WANG X.K., *Chem. Eng. J.*, 316 (2017), 419.
- [9] SUN M.J., SONG G.Q., LIU J.J., CHEN H.M., NIE F.Q., *RSC Adv.*, 7 (2017), 13637.
- [10] YANG Q.M., ZHAO L., XU X., XU L., LUO Y.Z., *Nat. Commun.*, 2 (2011), 381.
- [11] HUANG M., MI K., ZHANG J.H., LIU H.L., YU T.T., YUANG A.H., KONG Q.H., XIONG S.L., *J. Mater. Chem. A*, 5 (2017), 266.
- [12] MAQBOOL Q., SINGH C., JASH P., PAUL A., SRIVASTAVA A., *Chem. Eur. J.*, 23 (2017), 24216.
- [13] FAN H.L., NIU R.T., DUAN J.Q., LIU W., SHEN W.Z., *ACS Appl. Mater. Int.*, 8 (2016), 19475.
- [14] BARKAOUI S., HADDADOU M., DHAOUADI H., RAOUAFI N., TOUATI F., *J. Solid State Chem.*, 228 (2015), 26.
- [15] CHIU J.M., LIN L.Y., YEH P.H., LAI C.Y., TENG K., TU C.C., YANG S.S., YU J.F., *RSC Adv.*, 5 (2015), 83383.
- [16] RANAWEERA C.K., WANG Z., ALQURASHI E., KAHOL P.K., DVOMIC P.R., GUPTA B.K., RAMASAMY K., MOHITE A.D., GUPTA G., GUPTA R.K., *J. Mater. Chem. A*, 4 (2016), 9014.
- [17] JUSTIN P., RAO G.R., *Int. J. Hydrogen Energ.*, 35 (2010), 9709.
- [18] LIN J.Y., CHOU S.W., *RSC Adv.*, 3 (2013), 2043.
- [19] YOU B., JIANG N., SHENG M.L., SUN Y.J., *Chem. Commun.*, 51 (2015), 4252.
- [20] XIE D.Y., JIANG Q., FU G.G., DONG Y., KANG X.M., CAO W., ZHAO Y., *Rare Metal Mat. Eng.*, 30 (2011), 94.
- [21] ZHANG Y.F., *Mater. Sci.-Poland*, 35 (2017), 188.
- [22] LI H. J., SUN L.M., LIU Z.H., *Acta Crystallogr. E*, 62 (2006), 2522.
- [23] COULDWELL M.C., HOUSE D.A., PENFOLD B.R., *Inorg. Chim. Acta*, 13 (1975), 61.
- [24] WANG P., GUO Y.F., ZHAO C.W., YAN J.J., LU P., *Appl. Energ.*, 201 (2017), 34.
- [25] KHAN M.A., KANG Y.M., *Mater. Lett.*, 156 (2015), 209.
- [26] MAHFOUZ M.G., GALHOUM A.A., GOMAA N.A., ABDELREHEM S.S., ATIA A.A., VINCENT T., GUIBAL E., *Chem. Eng. J.*, 262 (2015), 198.
- [27] XING J.C., ZHU Y.L., ZHOU Q.W., ZHENG X.D., JIAO Q.J., *Electrochim. Acta*, 136 (2014), 550.
- [28] TAO F., ZHAO Y.Q., ZHANG G.Q., LI H.L., *Electrochem. Commun.*, 9 (2007), 1282.
- [29] ZHANG C., CHEN Q., ZHAN H., *ACS Appl. Mater. Inter.*, 8 (2016), 22977.
- [30] JIANG C., ZHAO B., CHENG J.Y., LI J.Q., ZHANG H.J., TANG Z.H., YANG J.H., *Electrochim. Acta*, 173 (2015) 399.
- [31] LEE J.W., AHN T., SOUNDARARAJAN D., KO J.M., KIM J.D., *Chem. Commun.*, 47 (2011), 6305.
- [32] LIU B., YUAN H., ZHANG Y., ZHOU Z., SONG D., *J. Power Sources*, 79 (1999), 277.
- [33] XU Q., JIANG D.L., WANG T.Y., MENG S.C., CHEN M., *RSC Adv.*, 6 (2016), 55039.
- [34] ZHAO J., GUAN B., HU B., XU Z.Y., WANG D.W., ZHANG H.H., *Electrochim. Acta*, 230 (2017), 428.
- [35] CONG H.P., REN X.C., WANG P., YU S.H., *ACS Nano.*, 6 (2012), 2693.
- [36] HOSSEINI M.G., SHAHRYARI E., *J. Colloid Interf. Sci.*, 496 (2017), 371.
- [37] ZHANG Q.F., XU C.M., LU B.G., *Electrochim. Acta*, 132 (2014) 180.

Received 2017-08-05

Accepted 2018-04-14